Japanese Journal of Applied Physics 53, 04EH10 (2014) **REGULAR PAPER**
http://dx.doi.org/10.7567/JJAP.53.04EH10

Fundamental study of inorganic–organic hybrid scintillator using Pr:$Lu_3Al_5O_{12}$ and plastic scintillator

Kei Kamada[1,2], Shunsuke Kurosawa[3], Yuui Yokota[2], Takayuki Yanagida[4], Martin Nikl[5], and Akira Yoshikawa[1,2,3]

[1]*C&A Corporation, Sendai 980-8579, Japan*
[2]*New Industry Creation Hatchery Center, Tohoku University, Sendai 980-8579, Japan*
[3]*Institute for Material Reseach, Tohoku University, Sendai 980-8577, Japan*
[4]*Kyushu Institute of Technology, Kitakyushu 808-0196, Japan*
[5]*Institute of Physics AS CR, 16253 Prague, Czech Republic*

Received October 4, 2013; accepted December 24, 2013; published online March 25, 2014

Read out test of inorganic–organic hybrid scintillator; Pr:LuAG single crystal covered with plastic scintillator BC-499 is demonstrated. Emission peaks of the hybrid scintillator was observed around 430 nm, which suit to the sensitive wavelength of photomultiplier tube (PMT). The Pr:LuAG sample coated with BC-499 showed the better light output than the that of Pr:LuAG itself. Light output was increased up to 30% sing PMT (Hamamatsu R9800). Decay curve of the hybrid scintillator was also measured and successfully modeled. Corporation.

1. Introduction

Scintillator materials combined with photo detectors are used to detect high energy photons and particles, e.g., in X-ray computed tomography (CT), positron emission tomography (PET) and other medical imaging techniques, high energy and nuclear physics detectors, etc. In most of these applications, scintillators that possess properties such as high stopping power, high light yield, short decay time, and very good energy resolution should used. Moreover, it is important to match emission wavelength of a scintillator with the maximum of spectral sensitivity of the coupled photo-detector to optimize the light output. In the past decades, great effort was made to develop more efficient and fast scintillators to detect ionizing radiation.

Recently, single crystal $Lu_3Al_5O_{12}$:Pr (Pr:LuAG) has attracted attention because of its interesting properties such as Pr^{3+} 5d–4f emission at 310 nm wavelength, non-hygroscopic nature, high density (6.7 g/cm^3), high light output (around 20000 photons/MeV), very short decay time (20 ns), and good energy resolution (4.8% at 662 keV for a 10 × 10 × 10 mm Pr:LuAG sample).[1–18] Table I shows a comparison of Pr:LuAG and popular cerium-activated scintillators such as Ce:Lu_2SiO_5 (Ce:LSO),[19–21] (Lu,Y)AlO_3 (LuAP),[21–24] and Ce:$LaBr_3$.[24–27] Owing to this excellent properties, Pr:LuAG scintillator is attracting attention for γ-ray detectors for oil well logging and has potential applications in high-energy physics and medical field such as PET. In order to apply Pr:LuAG to γ-ray detection applications, we are making efforts to establish mass production of Pr:LuAG single crystals. As a result of our effort, 2-in.-diameter Pr:LuAG have been commercially available now.[7,11] However, as shown in Fig. 1, the position of its scintillation emission spectrum peaking around 311 nm does not match well the spectral sensitivity of the general photodetectors such as photomultiplier tubes (PMT).

Organic scintillators (plastics, liquids) on the contrary are composed of aromatic hydrocarbons. Plastic scintillators are non-fluid solutions consisting of fluorescent organic compounds dissolved in a solidified polymer matrix. Organic scintillators are made of low Z-elements and have a low density. Therefore, the main interaction mechanism is Compton scattering. The photoelectric effect is dominant only at low energies (typically below 20 keV). Because of the low density, more volume (thickness) is required to obtain reasonable detection efficiency. However, the relatively low cost of plastic scintillators more than compensates for this when large area detectors are required. The low intrinsic scintillation efficiency of organic scintillators results in rather weak pulses for X-ray/γ-ray energies below 100 keV. Standard plastic scintillators, such as BC-400 series (Saint-

Table I. Comparison between Pr:LuAG and popular cerium-activated scintillators.

	Pr:LuAG	LSO:Ce	LuYAP:Ce	$LaBr_3$:Ce
Light output (photons/MeV)	20000	38000	<20000	70000
Energy resolution at 662 keV (%)	4.6	8	6.8	3
Density (g/cm^3)	6.73	7.4	6.1–8	5.1
Effective Z	62.9	66	40–63	47
Emission wavelength (nm)	310	420	360	380
Decay time (ns)	~20	40	20	20

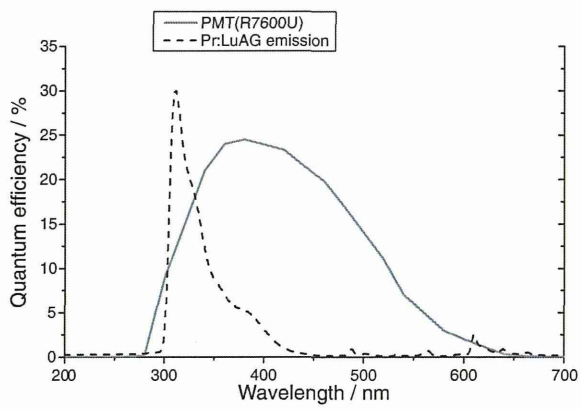

Fig. 1. Quantum efficiency of PMT (Hamamatsu R9800) and emission spectrum of Pr:LuAG.

Gobain),[28,29] have a light output which is about a factor of 2–4 lower than that of LYSO. Therefore, the main use of plastic scintillators for gamma detection is for gamma energies below 100 keV.

In this study, we have investigate the effect of covering the Pr:LuAG with plastic scintillators to shift the luminescence wavelength towards the region of higher spectral sensitivity of PMT.

2. Methods

2.1 Sample preparations

Pr:LuAG single crystals were grown using Czochralski (CZ) method[6,11] with an RF heating system in Furukawa. Pr concentration is 0.25 at. % (with respect to Lu). Crystal growth was carried out with the rotation rate of 8–12 rpm and growth rate was 1.0 mm/h. An automatic control system was used to control the crystal diameter. Crystals of approximately 100 mm in diameter and 100 mm long were grown from an Ir crucible. An Ar atmosphere was used to prevent Ir crucible from oxidization. The seed crystals were [100] oriented Pr:LuAG crystal. At the end of crystal growth process, the crystal was pulled above the melt and gradually cooled down to room temperature. Sample pieces were cut and polished into with $10 \times 10 \times 10\,mm^3$ size.

The plastic scintillator used in this system is an organic scintillator made of poly(vinyl toluene) base doped with aromatic additives to increase its scintillation efficiency. These plastic scintillators are available commercially in different nomenclature depending on the wavelength of the emission desired. In this study, a colorless transparent plastic scintillator nominated as BC-499 (Saint-Gobain), which have excitation peak at around 300 nm and emission peak at 430 nm with fast decay time of 2.1 ns, was selected as the candidate for the effective wavelength shifter of Pr:LuAG. As shown in Fig. 2, Pr:LuAG single crystal was coupled with BC499 thin film and five plane of the cubic crystal were covered with Teflon tape. One plane, which is faced towards the window of PMT (Hamamatsu R9800).

2.2 Optical, luminescence, and radiation response measurements

Absorption and photoluminescence spectra were obtained by a spectrophotometer (Hitachi U-4000) and fluorescence spectrophotometer (Hitachi F-4500), respectively. Radioluminescence spectra were obtained by a spectrofluorometer SR163 (ANDOR) using an X-ray tube (operated at 40 kV and 20 mA, Cu cathode).

To determine light yield, the energy spectra were collected under 662 keV γ-ray excitation (^{137}Cs source) using an amplifier with a shaping time of 0.5 μs, the PMT and a multichannel analyzer in the pulse height mode. Once the photo-absorption peak was detected, double Gaussian function was applied to fit the peak. In such analysis, the light yield and energy resolution were compared each other.

The decay time was also measured by using pico second pulse X-ray equipped streak camera system which was our original instrument.[30] The measured wavelength was set to be 420 nm for WLS applied Pr:LuAGs and 315 nm for Pr:LuAG, respectively. The averaged energy of emitted X-rays was 20 keV and the timing resolution was around 80 ps.

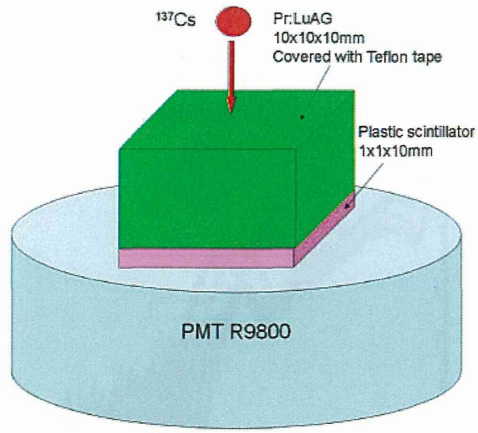

Fig. 2. (Color online) The geometry of the light output measurements.

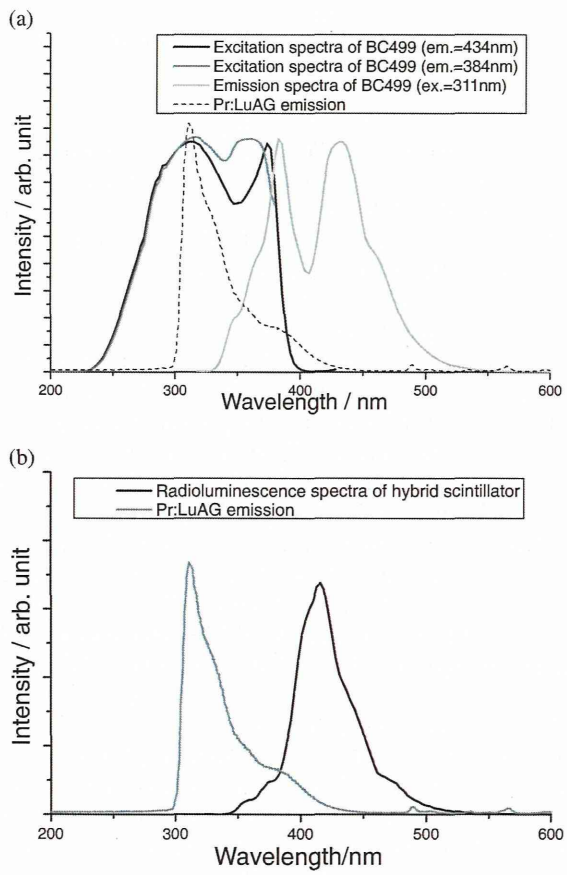

Fig. 3. (a) Excitation and emission spectra of BC499 and (b) radioluminescence spectra of the hybrid scintillator and Pr:LuAG itself.

3. Result and discussion

3.1 Luminescence measurements

Emission spectrum of BC-499 was measured at 310 nm excitation by Hitachi F-2700. As shown in Fig. 3(a), emission peaks at 384 and 434 nm ware observed. These emission peaks suit to sensitive wavelength of the PMT. Fluorescence spectrophotometer. Excitation spectra were also measured at 384 and 434 nm. E excitation peaks of BC-499 are well matched with the Pr:LuAG emission peak at 310 nm. Radioluminescence spectrum of hybrid scintillator

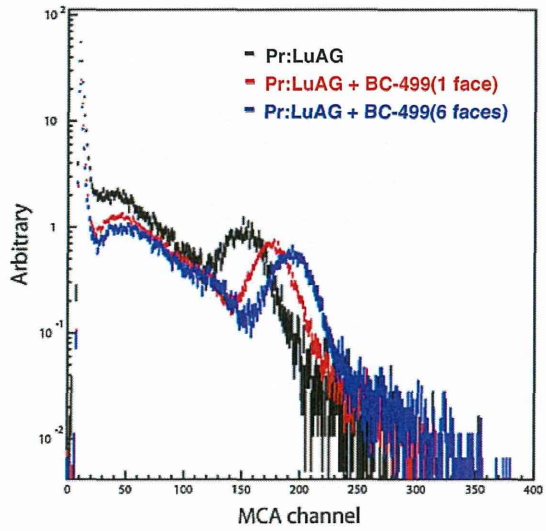

Fig. 4. (Color online) Energy spectra of Pr:LuAG itself and hybrid scintillators.

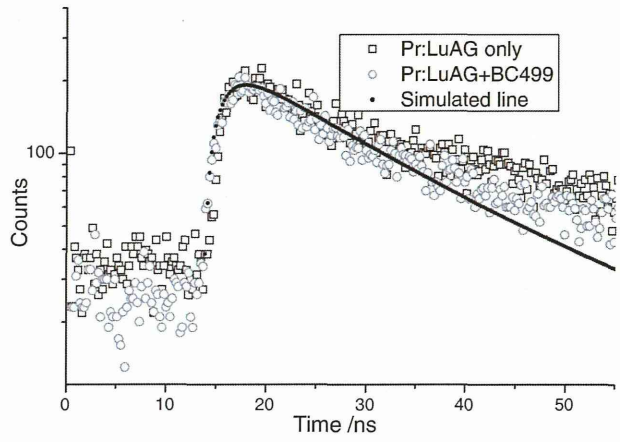

Fig. 5. Decay curves of Pr:LuAG itself and hybrid scintillator.

using Pr:LuAG and BC-499 was measured with a spectrofluorometer 199S (Edinburgh Instrument) using an X-ray tube (operated at 35 kV and 16 mA, Mo cathode). As shown in Fig. 3(b), emission wavelength of the hybrid scintillator successfully shifted to around 430 nm.

3.2 Light output measurements

Gamma ray response of Pr:LuAG coated with BC-499 on a face and all faces of the 10 mm cubic sample were measured under ^{137}Cs excitation at room temperature. Obtained energy spectra were shown in Fig. 4. Light output of one face and all faces coated hybrid scintillator ware 118 and 130%, respectively, higher than that of Pr:LuAG itself. Energy resolutions of Pr:LuAG itself, one face and all faces coated hybrid scintillator were 12.4, 10.1, and 10.3%, respectively. Shifting of Pr:LuAG emission towards the region of higher sensitivity of the used PMT by BC-499 could be an effective solution to improve light output and energy resolution.

3.3 Decay curve measurement

Let us suppose that all the photons from inorganic scintillator will reach to organic scintillator. We consider the case as a classical donor–accept radiative energy transfer, where the donors and acceptors are the Pr^{3+} and plastic scintillator emission centers, respectively. (N: excited state number at $t = 0$.) Decay curve of emission from Pr:LuAG due to Pr^{3+} 4f–5d transition was written as[1–11]

$$\frac{dN_i}{dt} = -\frac{1}{\tau_i} N_i \Leftrightarrow N_i(t) = N \exp\left(-\frac{t}{\tau_i}\right). \quad (1)$$

N_0 stands for the number of excited states in organic scintillator, Here, τ_0 is its decay time and α defines as ratio of absorbed photons by organic scintillator generated from inorganic scintillator. τ_i is decay time of inorganic scintillator. ε_i is luminescent efficiency:

$$\frac{dN_0}{dt} = \alpha \frac{\varepsilon_i N}{\tau_i} \exp\left(-\frac{t}{\tau_i}\right) - \frac{1}{\tau_0} N_0. \quad (2)$$

If the initial condition is $N_0(t = 0) = 0$,

$$N_0(t) = \alpha \frac{\varepsilon_i N \tau_0}{\tau_i - \tau_0} \left[\exp\left(-\frac{t}{\tau_i}\right) - \exp\left(-\frac{t}{\tau_0}\right)\right]. \quad (3)$$

When wavelength shifter works ideally, $\alpha = 1$ and

$$S_{\text{shifted}}(t) = \sigma_0 \frac{\varepsilon_i \varepsilon_0 N}{\tau_i - \tau_0} \left[\exp\left(-\frac{t}{\tau_i}\right) - \exp\left(-\frac{t}{\tau_0}\right)\right]. \quad (4)$$

Decay curves of the hybrid scintillator coated with BC-499 on all faces of the Pr:LuAG. Pr:LuAG itself and the hybrid scintillator were obtained at the range between 405 and 435 nm under the X-ray excitation. Experimentally obtained decay curves and simulated one using the above equation are shown in Fig. 5 with decay curve of the Pr:LuAG itself at the range between 300 and 460 nm. Decay time of Pr:LuAG and the BC-499 itself are $\tau_i = 18.7$ and $\tau_0 = 2.1$, respectively. These obtained decay time are used for the simulation. It is found that the simulated decay curve well reproduced the experimentally observed curve.

4. Conclusion

It is concluded that the hybrid scintillator realized with the Pr:LuAG scintillator covered by BC-499 can improve the scintillation performance when using the PMT. Emission wavelength of the hybrid scintillator successfully shifted to around 430 nm in which PMT have better quantum efficiency than that of 310 nm. In the case of the hybrid scintillator, light output was increased up to 130% compared to Pr:LuAG itself. Decay curve of the Pr:LuAG sample coupled with the WLS was also measured and successfully modeled.

Acknowledgements

This work is partially supported by (i) the funding program for next generation world-leading researchers, JSPS, (ii) Development of Systems and Technology for Advanced Measurement and Analysis, Japan Science and Technology Agency (JST), (iii) Adaptable and Seamless Technology Transfer Program through Target-driven R&D (A-STEP), JST, (iv) Japan Society for the Promotion of Science (JSPS) Grant-in-Aid for Exploratory Research (A.Y.), (v) JSPS Research Fellowships for Young Scientists (S. Kurosawa), and (vi) the Health Labour Sciences Research Grant, the Ministry of Health Labour and Welfare. In addition, we would like to thank following persons for their

support: Mr. Yoshihiro Nakamura in Institute of Multidisciplinary Research for Advanced Materials (IMRAM), Tohoku University and Mr. Hiroshi Uemura, Ms. Keiko Toguchi, Ms. Megumi Sasaki, and Ms. Yuka Takeda in IMR.

1) M. Nikl, H. Ogino, A. Yoshikawa, E. Mihokova, J. Pejchal, A. Beitlerova, A. Novoselov, and T. Fukuda, Chem. Phys. Lett. **410**, 218 (2005).
2) H. Ogino, A. Yoshikawa, M. Nikl, A. Krasnikov, K. Kamada, and T. Fukuda, J. Cryst. Growth **287**, 335 (2006).
3) M. Nikl, H. Ogino, A. Krasnikov, A. Beitlerova, A. Yoshikawa, and T. Fukuda, Phys. Status Solidi A **202**, R4 (2005).
4) H. Ogino, A. Yoshikawa, M. Nikl, K. Kamada, and T. Fukuda, J. Cryst. Growth **292**, 239 (2006).
5) K. Kamada, K. Tsutsumi, Y. Usuki, H. Ogino, T. Yanagida, and A. Yoshikawa, IEEE Trans. Nucl. Sci. **55**, 1488 (2008).
6) K. Kamada, T. Yanagida, Y. Usuki, and A. Yoshikawa, Nucl. Instrum. Methods Phys. Res., Sect. A **610**, 215 (2009).
7) K. Kamada, T. Yanagida, K. Tsutsumi, Y. Usuki, M. Sato, H. Ogino, A. Novoselov, A. Yoshikawa, M. Kobayashi, S. Sugimoto, and F. Saito, IEEE Trans. Nucl. Sci. **56**, 570 (2009).
8) L. Swiderski, M. Moszynski, A. Nassalski, A. Syntfeld-Kazuch, T. Szczesniak, K. Kamada, K. Tsutsumi, Y. Usuki, T. Yanagida, and A. Yoshikawa, IEEE Trans. Nucl. Sci. **56**, 1 (2009).
9) T. Kato, J. Kataoka, T. Nakamori, T. Miura, H. Matsuda, K. Sato, Y. Ishikawa, K. Yamamura, N. Kawabata, H. Ikeda, G. Sato, and K. Kamada, Nucl. Instrum. Methods Phys. Res., Sect. A **638**, 83 (2011).
10) K. Kamada, T. Yanagida, J. Pejchal, M. Nikl, T. Endo, K. Tsutsumi, Y. Fujimoto, A. Fukabori, and A. Yoshikawa, IEEE Trans. Nucl. Sci. **59**, 2126 (2012).
11) T. Yanagida, Y. Fujimoto, K. Kamada, D. Totsuka, H. Yagi, T. Yanagitani, Y. Futami, S. Yanagida, S. Kurosawa, Y. Yokota, A. Yoshikawa, and M. Nikl, IEEE Trans. Nucl. Sci. **59**, 2146 (2012).
12) M. Nikl, K. Kamada, S. Kurosawa, Y. Yokota, A. Yoshikawa, J. Pejchal, and V. Babin, Phys. Status Solidi **10**, 172 (2013).
13) K. Kamada, T. Yanagida, J. Pejchal, M. Nikl, T. Endo, K. Tsutumi, Y. Fujimoto, A. Fukabori, and A. Yoshikawa, IEEE Trans. Nucl. Sci. **59**, 2130 (2012).
14) K. Kamada, T. Yanagida, T. Endo, K. Tsutumi, M. Yoshino, J. Kataoka, Y. Usuki, Y. Fujimoto, A. Fukabori, and A. Yoshikawa, J. Cryst. Growth **352**, 91 (2012).
15) K. Kamada, T. Yanagida, S. Kurosawa, Y. Yokota, T. Endo, K. Tsutsumi, and A. Yoshikawa, IEEE Trans. Nucl. Sci. (in press) [DOI: 10.1109/TNS.2013.2278024].
16) W. Drozdowski, K. Brylew, M. E. Witkowski, A. J. Wojtowicz, K. Kamada, T. Yanagida, and A. Yoshikawa, Radiat. Meas. **56**, 80 (2013).
17) M. Nikl, A. Yoshikawa, K. Kamada, K. Nejezchleb, C. R. Stanek, J. A. Mares, and K. Blazek, Prog. Cryst. Growth Charact. Mater. **59**, 47 (2013).
18) K. Brylew, W. Drozdowski, M. E. Witkowski, K. Kamada, T. Yanagida, and A. Yoshikawa, Cent. Eur. J. Phys. **11**, 138 (2013).
19) C. L. Melcher and J. S. Schweitzer, IEEE Trans. Nucl. Sci. **39**, 502 (1992).
20) M. Kapusta, P. Szupryczynski, C. L. Melcher, M. Moszynski, M. Balcerzyk, A. A. Carey, W. Czarnacki, M. A. Spurrier, and A. Syntfeld, IEEE Trans. Nucl. Sci. **52**, 1098 (2005).
21) M. A. Spurrier, P. Szupryczynski, K. Yang, A. A. Carey, and C. L. Melcher, IEEE Trans. Nucl. Sci. **55**, 1178 (2008).
22) P. Lecoq and M. Korzhik, IEEE Trans. Nucl. Sci. **49**, 1651 (2002).
23) M. Moszyński, D. Wolski, T. Ludziejewski, M. Kapusta, A. Lempicki, C. Brecher, D. Wiśniewski, and A. J. Wojtowicz, Nucl. Instrum. Methods Phys. Res., Sect. A **385**, 123 (1997).
24) S. Weber, D. Christ, M. Kurzeja, R. Engels, G. Kemmerling, and H. Halling, IEEE Trans. Nucl. Sci. **50**, 1370 (2003).
25) M. Korzhik, A. Fedorov, A. Annenkov, A. Borissevitch, A. Dossovitski, O. Missevitch, and P. Lecoq, Nucl. Instrum. Methods Phys. Res., Sect. A **571**, 122 (2007).
26) K. S. Shah, J. Glodo, M. Klugerman, W. W. Moses, S. E. Derenzo, and M. J. Weber, IEEE Trans. Nucl. Sci. **50**, 2410 (2003).
27) J. Glodo, W. W. Moses, W. M. Higgins, E. V. D. van Loef, P. Wong, S. E. Derenzo, M. J. Weber, and K. S. Shah, IEEE Trans. Nucl. Sci. **52**, 1805 (2005).
28) Brillance 380 Data Sheet, Saint-Gobain Crystals (2013) [http://www.detectors.saint-gobain.com].
29) BC-400 Data Sheet, Saint-Gobain Crystals (2013) [http://www.detectors.saint-gobain.com/].
30) T. Yanagida, Y. Fujimoto, A. Yoshikawa, Y. Yokota, K. Kamada, J. Pejchal, V. Chani, N. Kawaguchi, K. Fukuda, K. Uchiyama, K. Mori, K. Kitano, and M. Nikl, Appl. Phys. Express **3**, 056202 (2010).

Read Out Test of Pr:LuAG Scintillator Coupled to Organic Wavelength Shifter Using Si Based Photodetectors

Kei Kamada, Takayuki Yanagida, Shunsuke Kurosawa, Yuui Yokota, Takanori Endo, Kousuke Tsutsumi, and Akira Yoshikawa

Abstract—**Functional possibilities of Pr:LuAG single crystal covered with plastic scintillators are demonstrated. Shift of luminescence wavelength of the hybrid scintillators towards the region of higher spectral sensitivity of photodetectors and radiation responses of the hybrid scintillators were investigated. The Pr:LuAG sample coated with bis-MSBPVD showed the better light output and energy resolution than the Pr:LuAG itself. Light output was increased up to 55% and energy resolution was also improved to 6.5%@662 keV using APD (Hamamatsu S8664-8220). In the case of MPPC (Hamamatsu S10362_33_050 3600 pixel-type), light output was increased up to 35% and energy resolution was also improved to 9.8%@662 keV. Decay curve of the Pr:LuAG sample coupled with the WLS was also measured and successfully modeled.**

Index Terms—**Crystals, luminescence, solid scintillation detectors.**

I. Introduction

SCINTILLATOR coupled to photo-detectors have been widely used in many fields including high energy physics, astrophysics, industrial defectscopy and medical imaging, especially in positron emission tomography (PET) [1]. In most of these applications, scintillators that possess properties such as high stopping power, high light yield, short decay time, and very good energy resolution should be used. Moreover, it is important to match emission wavelength of a scintillator with the maximum of spectral sensitivity of the coupled photo-detector to optimize the light output.

Recently, Pr:$Lu_3Al_5O_{12}$ (Pr:LuAG) has attracted attention because of its favorable combination of fast Pr^{3+} 5d-4f emission peaking at 311 nm, non-hygroscopic nature, high density (6.7 g/cm^3), high light output (around 20000 photon/MeV), very short decay time (20 ns), and good energy resolution (4.8% at 662 keV for a 10 × 10 × 10 mm^3 Pr:LuAG sample and a Hamamatsu R1791 PMT) [2]–[5]. It shows higher light yield and faster scintillation response in comparison with the Ce-doped LuAG [6], [7], even if the problem of the slow scintillation components due to shallow electron traps remains [8]. However, in case of the Pr:LuAG the position of its scintillation emission spectrum peaking around 311 nm does not fit well the spectral sensitivity of the photodetectors such as standard photomultiplier tube (PMT), avalanche photodiode (APD) and silicon photomultiplier (Si-PM)(Fig. 1).

In this study, we have investigated the effect of covering the Pr:LuAG with plastic scintillator to shift the luminescence wavelength towards the region of higher spectral sensitivity of the mentioned photodetectors.

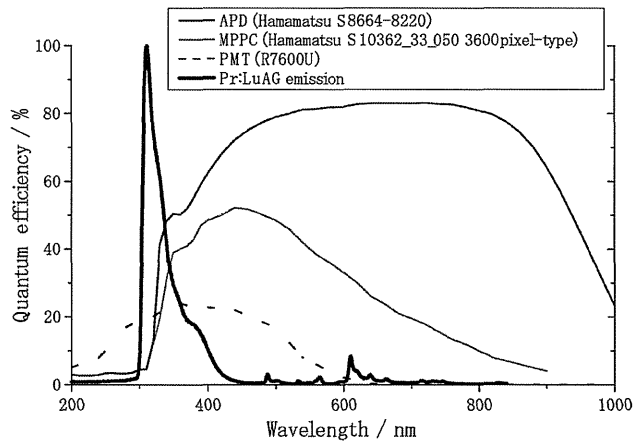

Fig. 1. Quantum efficiency of APD (Hamamats S8664-8220) and PMT (Hamamatsu R7600U), detection efficiency of MPPC (Hamamatsu S10362_33_050 3600 pixel-type) and emission spectrum of Pr:LuAG.

Manuscript received May 20, 2013; revised July 09, 2013 and July 26, 2013; accepted July 30, 2013. Date of publication December 03, 2013; date of current version February 06, 2014. This work was supported in part by the Japan Science and Technology Agency, Regional Research and Development Resources Utilization Program, in part by the Ministry of Education, Culture, Sports, Science, and Technology of the Japanese government, in part by a Grant-in-Aid for Young Scientists (A), 19686001 (AY), and (B), 15686001 (TY), and in part by the Shimadzu Science Federation.

K. Kamada is with the New Industry Creation Hatchery Center (NICHe), Tohoku University, Sendai 980-8579, Japan, and also with the C&A Corporation, Sendai 980-8579, Japan (e-mail: kamada@imr.tohoku.ac.jp).

T. Yanagida is with the Kyushu Institute of Technology, Fukuoka 808-0196 Japan.

S. Kurosawa is with the Institute for Material Research, Tohoku University, Sendai 980-8577, Japan.

Y. Yokota is with the New Industry Creation Hatchery Center (NICHe), Tohoku University, Sendai 980-8579, Japan.

T. Endo and K. Tsutsumii are with the Materials Research Laboratory, Furukawa Co. Ltd, Tsukuba 305-0856, Japan.

A. Yoshikawa is with the New Industry Creation Hatchery Center (NICHe), Tohoku University, Sendai 980-8579, Japan, also with the C&A Corporation, Sendai 980-8579, Japan, and also with the Institute for Material Research, Tohoku University, 980-8577 Sendai, Japan.

Digital Object Identifier 10.1109/TNS.2013.2278024

TABLE I
PLASTIC SCINTILLATORS INVESTIGATED IN THIS STUDY

	POPOP	DM-POPOP	Coum. 1	TB-PVD	PPO	Bis-MSB
Max. Emission Wavelength, nm	406	434	391	360	360	435
Excitation Wavelength at Max. Emission, nm	355	360	380	315	308	361
Decay time , ns	1.44	1.4	1-4	1.6	1.4	1.1

II. EXPERIMENTAL SET-UP AND SIMULATION

A. Sample Preparations

Plastic scintillators are commonly composed with a base polymer and luminescent dopants. In order to use plastic scintillators as wavelength shifters (WLSs), the matching of the absorption wavelength of luminescent dopants with the emission wavelength of the scintillator is important to achieve high conversion efficiency. Additionally, wavelength of converted photons emitted from WLS must be suitable for the sensitivity of the photodetectors.

Pr:LuAG single crystals were grown using Czochralski (CZ) method [3] with an RF heating system in Furukawa Co. Ltd. Pr concentration is 0.25 at. % (with respect to Lu). Crystal growth was carried out with the rotation rate of 8–12 rpm and growth rate was 1.0 mm/h. An automatic control system was used to control the crystal diameter. Crystals of approximately 100 mm in diameter and 100 mm long were grown from an Ir crucible. An Ar atmosphere was used to prevent Ir crucible from oxidation The seed crystals were [100] oriented Pr:LuAG crystal. At the end of crystal growth process, the crystal was pulled above the melt and gradually cooled down to room temperature.

Sample pieces were cut and polished into with $3 \times 3 \times 10$ mm^3 size. Polyvinyl-toluene was chosen as a base polymer for plastic scintillators because it is most widely used in plastic scintillators such as BC-499 (Saint-Gobain K.K.). In addition, BC-499 was good choice for coupling with Pr:LuAG scintillator according to the previous study [9], [10]. Six types of luminescent dopants, which have absorption peak around 300–380 nm and emission peak around 360–440 with fast decay time were selected in this work. Their main properties are presented in Table I according to experimental results and [11], [12].

Mixture solution of Polyvinyl-toluene, luminescent dopants and toluene was pasted on all surface of the Pr:LuAG samples. After evaporation of toluene, the samples were coated by the WLS with around 20 μm thickness.

B. Light Output and Decay Time Measurements

WLSs coated samples were covered with Teflon tape. The 3 × 3 mm face was coupled with photodetectors, APD (Hamamats S8664-8220), MPPC (Hamamatsu S10362_33_050 3600 pixel-type) and PMT (Hamamatsu R7600U) using an optical grease (OKEN 6262A). To determine light yield, the energy spectra were collected under 662 keV γ-ray excitation (^{137}Cs source). Once the photo-absorption peak was detected, double Gaussian function was applied to fit the peak. In such analysis, the light yield and energy resolution were compared each other.

The decay time was also measured by using pico second pulse X-ray equipped streak camera system which was our original instrument [9]. The measured wavelength was set to be 420 nm for WLS applied Pr:LuAGs and 315 nm for Pr:LuAG, respectively. The averaged energy of emitted X-rays was 20 keV and the timing resolution was around 80 ps.

C. Decay Time Simulation

We suppose that all the photons from inorganic scintillator will reach to organic scintillator. We consider the case as a classical donor-accept radiative energy transfer, where the donors and acceptors are the Pr^{3+} and plastic scintillator emission centers, respectively. (N: excited state number at t = 0)

$$\frac{dN_i}{dt} = -\frac{1}{\tau_i}N_i \Longleftrightarrow N_i(t) = N\exp\left(-\frac{t}{\tau_i}\right) \tag{1}$$

Number of photons per time is written as bellow. (Decay time of inorganic scintillator: τ_i, Luminescent efficiency: ε_i)

$$\frac{\varepsilon_i N}{\tau_i}\exp\left(-\frac{t}{\tau_i}\right) \tag{2}$$

N_0 stands for the number of excited states in organic scintillator, τ_0 is its decay time and α defines as ratio of absorbed photons by organic scintillator generated from inorganic scintillator.

$$\frac{dN_o}{dt} = \alpha\frac{\varepsilon_i N}{\tau_i}\exp\left(-\frac{t}{\tau_i}\right) - \frac{1}{\tau_o}N_o \tag{3}$$

If the initial condition is N_o (t = 0) = 0,

$$N_o(t) = \alpha\frac{\varepsilon_i N\tau_o}{\tau_i - \tau_o}\left[\exp\left(-\frac{t}{\tau_i}\right) - \exp\left(-\frac{t}{\tau_o}\right)\right] \tag{4}$$

When e_0 is defined as the luminescent efficiency of plastic scintillator, the number of photons, which will arrive at photodetector will be as follows:

$$\varepsilon_i(1-\alpha)\frac{1}{\tau_i}N_i + \varepsilon_o\frac{1}{\tau_o}N_o = (1-\alpha)\frac{\varepsilon_i N}{\tau_i}\exp\left(-\frac{t}{\tau_i}\right) + \alpha\frac{\varepsilon_i\varepsilon_o N}{\tau_i - \tau_o}\left[\exp\left(-\frac{t}{\tau_i}\right) - \exp\left(-\frac{t}{\tau_o}\right)\right] \tag{5}$$

When σ_i is defined as the efficiency of detection of photodetector with inorganic scintillator, ε_i is defined as the efficiency of detection at photodetector with organic scintillator, the time profile of photo-electron response will be shown as below.

$$\sigma_i\varepsilon_i(1-\alpha)\frac{1}{\tau_i}N_i + \sigma_o\varepsilon_o\frac{1}{\tau_o}N_o = \sigma_i(1-\alpha)\frac{\varepsilon_i N}{\tau_i}\exp\left(-\frac{t}{\tau_i}\right) + \sigma_o\alpha\frac{\varepsilon_i\varepsilon_o N}{\tau_i - \tau_o}\left[\exp\left(-\frac{t}{\tau_i}\right) - \exp\left(-\frac{t}{\tau_o}\right)\right] \tag{6}$$

When wavelength shifter works ideally, $\alpha = 1$ and

$$S_{shifted}(t) = \sigma_o\frac{\varepsilon_i\varepsilon_o N}{\tau_i - \tau_o}\left[\exp\left(-\frac{t}{\tau_i}\right) - \exp\left(-\frac{t}{\tau_o}\right)\right] \tag{7}$$

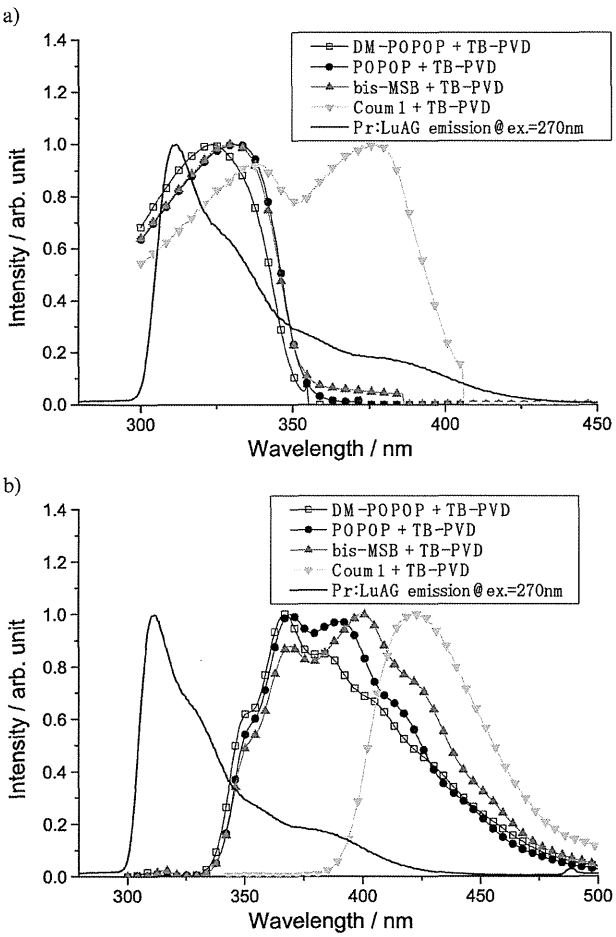

Fig. 2. a) Excitation spectra measured for the emission maxima of the WLSs and b) emission spectra of the WLSs s at 270 nm excitation.

If the wavelength shifter is not used,

$$S_{as\ emitted}(t) = \sigma_i \frac{\varepsilon_i N}{\tau_i} \exp\left(-\frac{t}{\tau_i}\right) \tag{8}$$

III. Results and Discussion

A. Luminescence Measurements

Excitation spectra measured for the maxima of emission bands of the WLSs themselves were measured by Hitachi F-2700 Fluorescence Spectrophotometer. As shown in Fig. 2(a), excitation peaks of the plastic scntillator are well matched with the Pr:LuAG emission peak. Because 310 nm emission of Pr:LuAG shows maximum excitation peak at 270 nm, emission spectra of the WLSs themselves were measured with excitation at 270 nm by Hitachi F-2700 Fluorescence Spectrophotometer Emission peaks were observed around 360–400 nm, which suit to the sensitive wavelength of mentioned Si based photodetectors. Radioluminescence spectra were measured with a Spectrofluorometer 199S (Edinburgh Instrument) using an X-ray tube (operated at 35 kV and 16 mA, Mo cathode). As shown in Fig. 3, emission wavelength of the WLSs coated samples successfully shifted to around 400 nm.

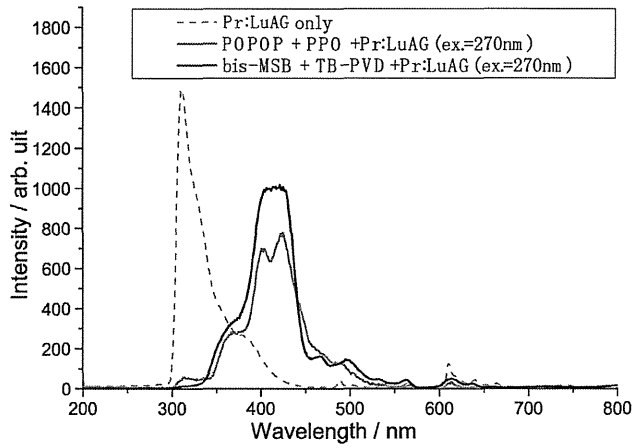

Fig. 3. Photoluminescence spectra of the WLSs coated and non-coated samples for an excitation at 270 nm.

B. Light Output Measurements

Gamma ray response of the Pr:LuAG sample coated with the WLSs was measured under ^{137}Cs excitation at room temperature. Obtained light yields, relative light outputs and energy resolutions are shown in Table II. Light yields were calculated with considering light yield of the Pr:LuAG standard (18000 photon/MeV) [4], [5], their positions of photo peaks measured using the APD and quantum efficiency of the APD at each emission wavelength (15%@310 nm, 50%@390 nm and 70%@420 nm). The sample coated with bis-MSB+TB-PVD containing WLS showed the best result at the point view of light output and energy resolution even though its light yield was lower than that of Pr:LuAG itself. Examples of the obtained energy spectra using the APD are shown in Fig. 4. In this case the light output was increased up to 55% and energy resolution was also improved to 6.5%@662 keV. Shifting of the Pr:LuAG emission towards the region of higher sensitivity of the used photodetector by WLSs could be an effective solution to increase the light output of such a scintillation detector.

C. Experimental Investigation of Decay Curve

Decay curves of the sample coated with bis-MSB+TB-PVD containing WLS and the WLS itself were obtained at the range between 405 and 435 nm under the X-ray excitation. Experimentally obtained decay curves and simulated one using the equations described in Section II-C are shown in Fig. 5 and compared to decay curve of the sample without WLS at the range between 300 and 460 nm. Decay time of the sample without WLS and the WLS itself are $\tau_i = 17.2$ and $\tau_0 = 1.6$ ns, respectively. These obtained decay time are used for the simulation. It is found that the simulated decay curve well reproduced the experimentally observed curve.

IV. Conclusions

It is concluded that the wavelength shifter realized with the Pr: LuAG scintillator covered by a tailored WLS can improve the scintillation performance when using the APD and MPPC. The Pr:LuAG sample coated with bis-MSB+TB-PVD containing WLS showed the better light output and energy

TABLE II
GAMMA RAY RESPONSE OF THE WLSs COATED SAMPLES USING THE APD AND MPPC

		APD		MPPC	
	Light yield	Relative Light yield	E.R. 662keV /%	Relative Light yield	E.R. 662keV /%
Without WLS	18000	1.00	8.1	1.00	11.2
PPO+POPOP	9600	1.34	7.3	1.32	10.3
PPO+bis-MSB	9700	1.35	7.4	1.22	10.5
PPO+DM-POPOP	8700	1.22	7.6	1.34	10.8
PPO+Coum1	5400	1.05	8.4	0.98	11.9
TB-PVD+POPOP	9300	1.30	7.5	1.23	11.0
TB-PVD+bis-MSB	11000	1.55	6.5	1.35	9.8
TB-PVD+DM-POPOP	9500	1.32	6.8	1.25	10.5-
TB-PVD +Coum1	5700	1.11	8.3	1.03	11.4

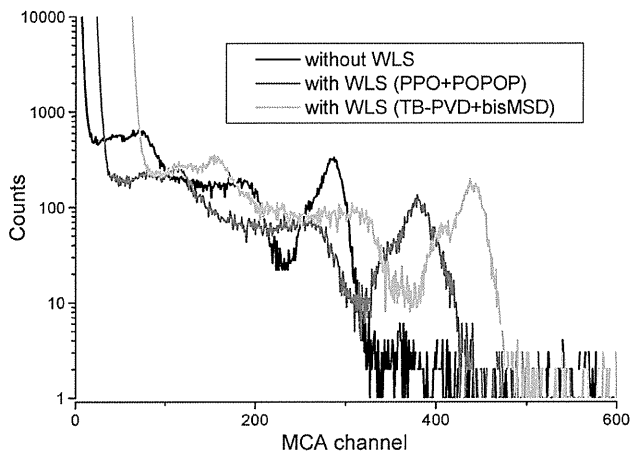

Fig. 4. Comparison of energy spectra of the sample coated with WLS and without WLS using the APD.

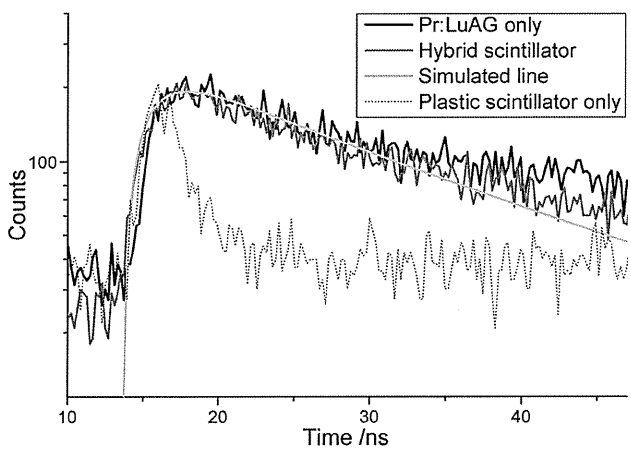

Fig. 5. Experimental decay curve and simulated one using the eq. (7).

resolution than the Pr:LuAG itself. Light output was increased up to 55% and energy resolution was also improved to 6.5%@662 keV. In the case of the MPPC, light output was increased up to 35% and energy resolution was also improved to 9.8%@662 keV.

Decay curve of the Pr:LuAG sample coupled with the WLSs was measured and successfully modeled.

APPENDIX

The following abbreviations were used in the present paper:

PPO	2,5-phenyloxzolyl
TB-PVD	2-(4-tertbutylphenyl)-5-(4-biphenyl)-oxadiazol)-1,3,4;
POPOP	1,4-di-2-(5-phenyloxzolyl);
Coum 1	diethylamino-4-methylcoumarin;
Bis-MSB	p-bis(o-methylstyryl) benzene
DM-POPOP	1,4-bis-(4-methyl-5-phenylaxazolyl-2-yl)-benzene

ACKNOWLEDGMENT

The authors would thank M. Nikl for useful discussions.

REFERENCES

[1] M. Nikl, "Scintillation detectors for X-rays," *Meas. Sci. Technol.*, vol. 17, pp. R37–R54, 2006.
[2] M. Nikl, H. Ogino, A. Krasnikov, A. Beitlerova, A. Yoshikawa, and T. Fukuda, "Photo- and radioluminescence of Pr-doped $Lu_3Al_5O_{12}$ single crystal," *Phys. Status Solidi A*, vol. 202, pp. R4–R6, 2005.
[3] K. Kamada, K. Tsutsumi, Y. Usuki, H. Ogino, T. Yanagida, and A. Yoshikawa, "Crystal growth and scintillation properties of 2-inch-diameter Pr : Lu3Al5O12 (Pr:LuAG) single crystal," *IEEE Trans. Nucl. Sci.*, vol. 55, no. 3, pp. 1488–1491, Jun. 2008.
[4] W. Drozdowski, P. Dorenbos, J. T. M. de Haas, R. Drozdowska, A. Owens, and K. Kamada *et al.*, "Scintillation properties of praseodymium activated Lu3Al 5O12 single crystals," *IEEE. Nucl. Trans. Sci.*, vol. 55, no. 4, pp. 2420–2424, Aug. 2008.
[5] L. Swiderski, M. Moszynski, A. Nassalski, A. Syntfeld-Kazuch, T. Szczesniak, and K. Kamada *et al.*, "Scintillation properties of praseodymium doped LuAG scintillator compared to cerium doped LuAG, LSO and LaBr3," *IEEE Trans. Nucl. Sci.*, vol. 56, no. 4, pp. 2499–2505, Jun. 2009.
[6] M. Nikl, E. Mihokova, J. A. Mares, A. Vedda, M. Martini, and K. Nejezchleb *et al.*, "Traps and timing characteristics of. LuAG:Ce scintillator," *Phys. Stat. Sol. (b)*, vol. 181, no. 1, pp. R10–R12, 2000.
[7] J. A. Mares, A. Beitlerova, M. Nikl, N. Solovieva, C. D'Ambrosio, and K. Blazek *et al.*, "Scintillation response of Ce-doped or intrinsic scintillating crystals in the range up to 1MeV," *Radiation Meas.*, vol. 38, pp. 353–357, 4 2004.
[8] M. Nikl, A. Vedda, M. Fasoli, I. Fontana, V. V. Laguta, and E. Mihokova *et al.*, "Shallow traps and radiative recombination processes in Lu3Al5O12:Ce single crystal scintillator," *Phys. Rev. B*, vol. 76, no. 19, pp. 195121–195126, 2007.
[9] A. Yoshikawa, T. Yanagida, Y. Yokota, K. Kamada, Y. Usuki, and M. Nikl, "Functional possibilities of inorganic-organic hybrid scintillator; Pr: LuAG scintillator covered with plastic scintillator," in *Proc. IEEE NSS MIC 2009, Conf. Rec.*, pp. 1524–1526.
[10] T. Yanagida, Y. Fujimoto, A. Yoshikawa, Y. Yokota, K. Kamada, and J. Pejchal *et al.*, "Development and performance test of picosecond pulse X-ray excited streak camera system for scintillator characterization," *Appl. Phys. Express*, vol. 3, pp. 056202–056206, 2010.
[11] L. A. Andryhchenko and B. V. Grinev, "Organosilicon materials for scintillation detectors of ionizing radiation," *Instrum. Exp. Tech.*, vol. 41, p. 447, 1998.
[12] L. A. Andryustchenko, A. M. Kudin, V. I. Goriletsky, B. G. Zaslavsky, D. I. Zosim, T. A. Charkina, and L. N. Trefilova *et al.*, "Functional possibilities of organosilicon coatings on the surface of CsI-based scintillators," *Nucl. Instrum. Meth. . A*, vol. 486, pp. 40–47, 2002.

Optical Materials xxx (2014) xxx–xxx

Contents lists available at ScienceDirect

Optical Materials

journal homepage: www.elsevier.com/locate/optmat

Cz grown 2-in. size Ce:$Gd_3(Al,Ga)_5O_{12}$ single crystal; relationship between Al, Ga site occupancy and scintillation properties

Kei Kamada [a,b,*], Shunsuke Kurosawa [c], Petr Prusa [d], Martin Nikl [d], Vladimir V. Kochurikhin [b], Takanori Endo [e], Kousuke Tsutumi [e], Hiroki Sato [e], Yuui Yokota [a], Kazumasa Sugiyama [c], Akira Yoshikawa [a,b,c]

[a] Tohoku University, New Industry Creation Hatchery Center, 6-6-10 Aoba, Aramaki, Aoba-ku, Sendai, Miyagi 980-8579, Japan
[b] C&A Corporation, T-Biz, 6-6-10 Aoba, Aramaki, Aoba-ku, Sendai, Miyagi 980-8579, Japan
[c] Tohoku University, Institute for Material Reseach, 2-1-1 Katahira Aoba-ku, Sendai, Miyagi 980-8577, Japan
[d] Institute of Physics AS CR,16253 Prague, Czech Republic
[e] Materials Research Laboratory, Furukawa co. ltd, 1-25-13, Kannondai, Tsukuba 305-0856, Japan

ARTICLE INFO

Article history:
Available online xxxx

Keywords:
Scintillator
Single crystal growth

ABSTRACT

2-in. size Ce 1%:$Gd_3(Al_{1-x}Ga_x)_5O_{12}$ (GAGG) single crystals with various Ga concentration of $x = 2$, 2.4, 2.7 and 3 were grown by the Czochralski (Cz) method. Light yield has maximum value of 58,000 photon/MeV at $x = 2.7$ Ga concentration. Energy resolution was improved with decreasing Ga concentration and $x = 2.4$ sample showed best energy resolution of 4.2%@662 keV. The dependence of scintillation properties on crystal structure and Al–Ga was discussed.

1. Introduction

Materials, which has garnet structure are promising candidates for scintillator applications, because of well-developed manufacturing technology as laser crystals. As it has optical transparency and has easy doping by rare-earth elements, it is considered for other applications, such as magneto-optics. After a decade of R&D of the $Lu_3Al_5O_{12}$-based single crystal scintillators, new material concept was defined, based on multicomponent $(Gd,RE)_3(Ga,Al)_5O_{12}$ host, Re = Lu, Y. Doped by Ce^{3+}, the Gd- and Ga rich host compositions showed amazingly high light yield up to almost 50,000 photon/MeV [1–8] which is the value exceeding by 30–40% the best LYSO:Ce materials ever seen. Recently, our group reported about Ce:$Gd_3Al_2Ga_3O_{12}$ (GAGG) single crystal and scintillation response of about ~90 ns at emission around 520 nm, prospective light yield of about 46,000 photon/MeV, and density of 6.63 g/cm^3 [2–4]. This multicomponent garnet Ce:$Gd_3(Ga,Al)_5O_{12}$ single crystals show very interesting features. The composition, which shows higher light yield, is not the same as that of higher energy resolution. Light yield and energy resolution has dependence on Al–Ga ratio. Moreover, when it crystallized, the initial phase has also strong dependence on Al–Ga ratio.

In this presentation, 2-in. size Ce 1%:$Gd_3(Al_{1-x}Ga_x)_5O_{12}$ (GAGG) single crystals with various Ga concentration of $x = 2$, 2.4, 2.7 and 3 were grown by the Czochralski (Cz) method using an RF heating system. Scintillation properties such as light yield and decay time were also evaluated. The dependence of scintillation properties on crystal structure and Al–Ga was discussed.

2. Experimental

2.1. Sample preparations

Stoichiometric mixtures of 4 N CeO_2, Gd_2O_3, β-Ga_2O_3 and α-Al_2O_3 powders (High Purity Chemicals Co.) were used as starting material. Nominally, Gd^{3+} site was substituted by Ce^{3+} according to the formula of $(Ce_{0.01}Gd_{0.99})_3Al_{5-x}Ga_xO_{12}$. Ce:GAGG ($x = 2$, 2.4, 2.7 and 3) single crystals were grown by means of the Cz method using an RF heating system. The rotation rate was 4–12 rpm and the growth rate was 1.0 mm/h. An automatic diameter control system using crystal weighing was applied to control the growth parameters. Crystals were grown from a 50 mm diameter Ir crucible under Ar with adding 30% of CO_2 atmosphere to prevent evaporation of gallium oxide. The seed crystal was a [100] oriented Ce:GAGG crystal. After the completion of the crystal growth, the crystal

* Corresponding author at: Tohoku University, New Industry Creation Hatchery Center, 6-6-10 Aoba, Aramaki, Aoba-ku, Sendai, Miyagi 980-8579, Japan. Tel.: +81 22 215 2214.
E-mail address: kamada@c-and-a.jp (K. Kamada).

http://dx.doi.org/10.1016/j.optmat.2014.04.001
0925-3467/

was removed from the melt and was gradually cooled down to room temperature.

2.2. Gamma-ray response measurement procedure

Light yield measurements were performed by using an avalanche photodiode (PD) (Hamamatsu, S8650) and APD (Hamamatsu S8664-55). Sample pieces with dimensions of 5 × 5 × 5 mm were cut from the grown single crystal, all surfaces were chemically polished. The samples were surrounded by $BaSO_4$ based reflector and optically coupled to the APD (Hamamatsu, S8664-55). The light yield (LY) of the sample was calibrated from the ^{55}Fe direct irradiation peak to APD. For the decay time measurement the same setup with a photomultiplier tube (PMT Hamamatsu R7600U-200 and digital oscilloscope TD5032B were used. Non-proportionality was determined by amplitude spectroscopy of scintillation response induced by gamma rays (Mares et al., 2007). Scintillation crystal is covered by teflon tape to ensure efficient light collection, and optically coupled to a hybrid photo-multiplier (HPMT) model DEP PPO 475B. Signal from HPMT is processed by spectroscopy amplifier ORTEC model 672 and multichannel-buffer ORTEC 927TM. Pulse height spectrum is displayed on a PC. Several gamma ray emitting radionuclide sources were used to induce a scintillation response: ^{137}Cs (661.6 keV), ^{22}Na (511 keV,1274 keV), ^{241}Am (59.54 keV, 13.95 keV), ^{210}Pb (46.54 keV,10.84 keV), ^{109}Cd (88.04 keV, 22.16 keV), and ^{133}Ba (81.0 keV,160.6 keV, 276.4 keV, 302.9 keV, 356.0 keV, and 383.9 keV)(Ekström and Firestone, 2004). Only selection of ^{133}Ba lines is presented for many samples due to non-negligible interference.1274 keV line of ^{22}Na is not presented because of experimental setup saturation.

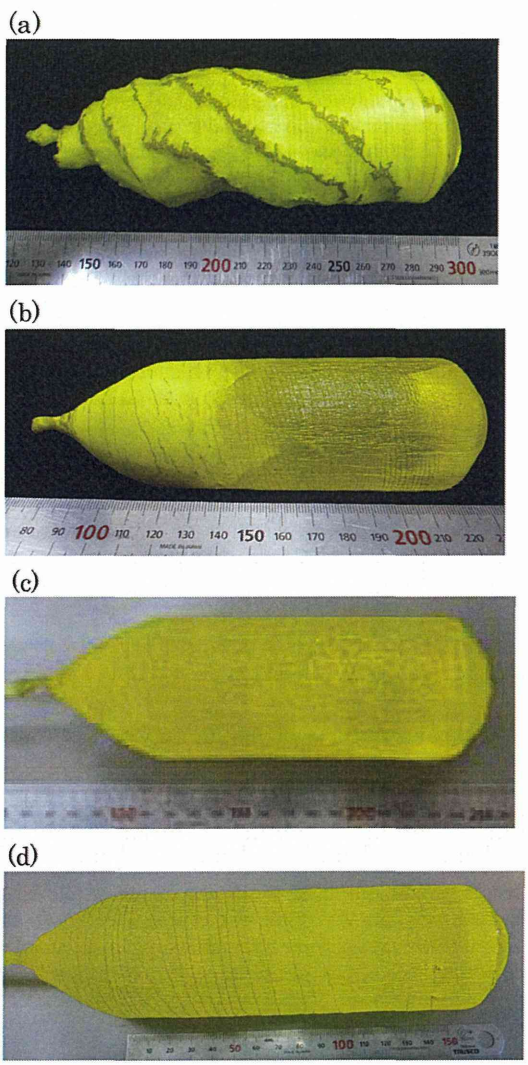

Fig. 1. Photographs of Ce:GAGG with Ga concentrations of x = (a) 2.0, (b) 2.4, (c) 2.7 and (d) 3.0.

3. Result and discussion

3.1. Crystal growth

Ce 1% doped GAGG (x = 2, 2.4, 2.7, and 3) crystals with a diameter of 50 mm and length of 80–120 mm were grown. The grown crystals looked slightly cloudy because of the rough surface caused by gallium oxide evaporation or thermal etching (see Fig. 1). Metallic stripes on the crystal surfaces were identified as Ir deposit comes from oxidation of the crucible. Powder X-ray diffraction (XRD) was performed to identify the phase of grown crystals. As shown in Fig. 2, beginning part of x = 2.0 and 2.4 had mixture phases of garnet and perovskite. This result is good agreement with previous report [9]. Single garnet phase appeared at the end part because of the increasing of Ga concentration due to Ga segregation. The crystals of x = 2.7 and 3 showed single garnet phase in whole crystals.

Quantitative chemical analysis of the crystals for the Ce content along the growth direction was performed by electron probe microanalysis (EPMA; JXA-8621MX, JEOL). So called ZAF correction was used, where Z stands for atomic number, A for absorption correction factor and F for fluorescence correction factor, respectively. The Ga distributions of Ce:GAGG (x = 2.4 and 2.7) along the growth direction are shown in Fig. 2. The solidification fractions (g) of the grown x = 2.4 and 2.7 crystals were 0.42 and 0.43, respectively. Here g is described as follows:

$$g = (\text{mass of solidified part})/(\text{total mass of starting raw material in the crucible})$$

Segregation coefficients of Ga were k_{eff} = 0.92 and 0.93 in x = 2.4 and 2.7 crystals. Secondary perovskite phase was observed in the part below Ga concentration of 2.3. This result is good agreement of previous reports [2,3,10].

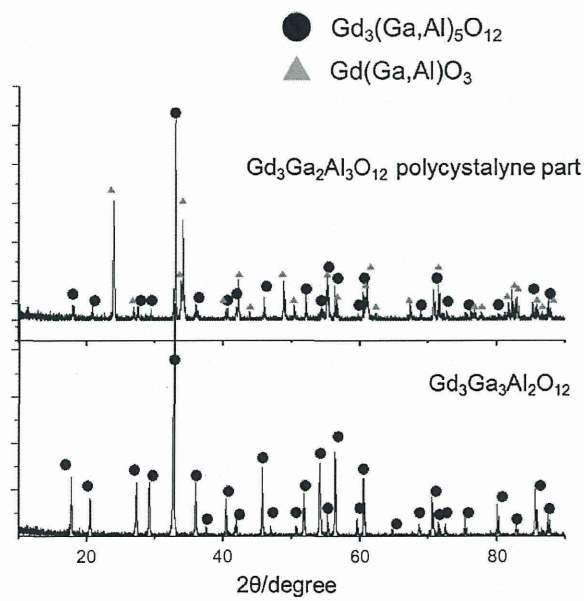

Fig. 2. Results of powder XRD on the grown x = 2.0 and x = 3.0 Ce:GAGG crystals.

Please cite this article in press as: K. Kamada et al., Opt. Mater. (2014), http://dx.doi.org/10.1016/j.optmat.2014.04.001